

UC Riverside

UCR Honors Capstones 2017-2018

Title

Hunting High and Low: Analyzing Techniques and Developing Strategies to Search for Supersymmetry at the Large Hadron Collider

Permalink

<https://escholarship.org/uc/item/39m0c6bh>

Author

Penafiel, Louis

Publication Date

2018-04-01

By

A capstone project submitted for
Graduation with University Honors

University Honors
University of California, Riverside

APPROVED

Dr.
Department of

Dr. Richard Cardullo, Howard H Hays Jr. Chair and Faculty Director, University Honors
Interim Vice Provost, Undergraduate Education

Abstract

Acknowledgments

Table of Contents

Abstract.....	ii
Acknowledgments.....	iii

1 Introduction

Dark matter composes more than 80 percent of the total mass in the universe [1]. However, our current understanding of physics does not properly explain dark matter, making it one of the most actively researched programs in physics. Our current understanding is based on the Standard Model of particle physics (SM), which explains the fundamental particles and their interactions, shown in **Fig: 1**. Though the SM is one of the most successful theories in physics, it does not explain three fundamental issues. First, there has to be an implausible level of fine tuning of SM parameters in order for the experimental value of the Higgs boson mass to be given. This implausibility is what we call the hierarchy problem. Second, the convergence of the strong, electromagnetic, and weak forces at a very high energy scale is not required by the Standard Model, not allowing for Grand Unification. Lastly, as the Standard Model is a self-contained list of particles and interactions, dark matter particles are not included, so the existence of dark matter is not explained by the SM [6]. Therefore, the SM requires extensions.

1.1 Supersymmetry

One of these extensions is supersymmetry (SUSY), which introduces particles called superpartners and their interactions [11]. The particles are basically another copy of the SM, with a boson in the SM being a fermion in SUSY and vice versa, shown in **Fig: 2**. SUSY can explain the three fundamental issues in physics. First, SUSY can explain the hierarchy problem with the interactions of the superpartners, explained in **Fig: 3**. Second, it allows for the possibility of Grand Unification. Lastly, it can explain the existence of dark matter, since the lightest supersymmetric particle (LSP) is a neutral, stable, weakly-interacting particle, similar to what we expect of dark matter. Hence, the search for SUSY is an important ongoing endeavor at CERN's Large Hadron Collider (LHC)–

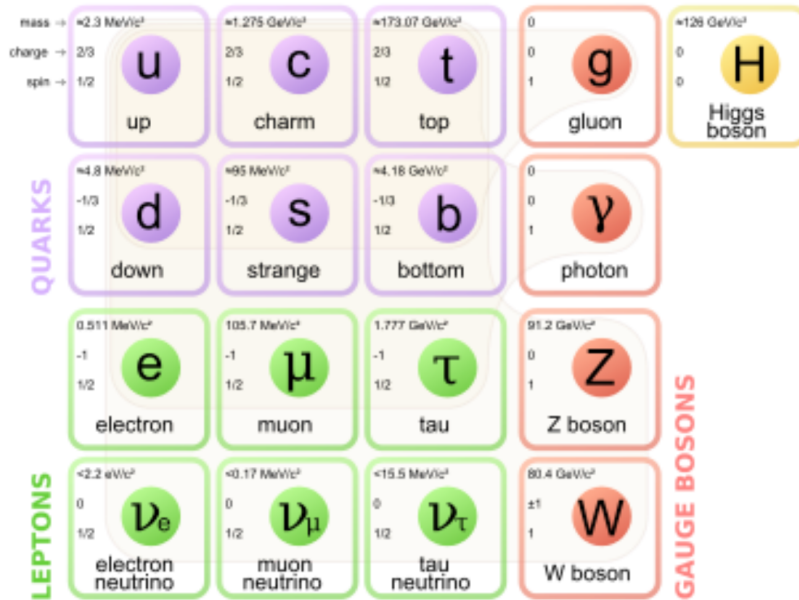


Figure 1: The Standard Model of particle physics showing the list of particles and their properties. The SM is separated into quarks, leptons, gauge bosons, and the Higgs boson. Created by Dave Fehling.

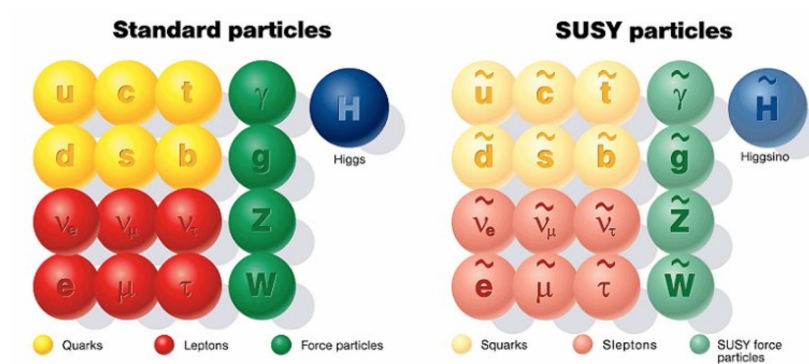


Figure 2: The Standard Model of particle physics along with the supersymmetric copy of the particles. Created by Pauline Gagnon

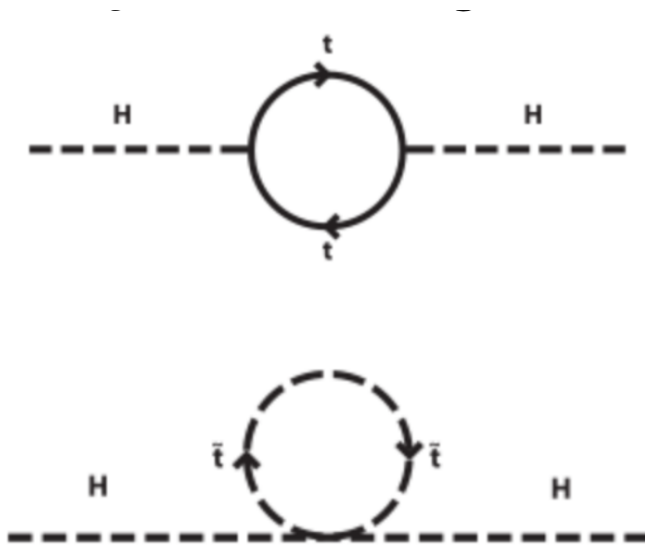


Figure 3: The hierarchy problem is that the low mass of the Higgs boson causes the top interaction to have quantum corrections around the order of the Planck mass, which is many orders of magnitude higher compared to the mass of the Higgs boson. By introducing supersymmetric particles, new interactions, such as the one in the bottom are introduced, effectively cancelling the quantum corrections. Created by user VermillionBird in Wikipedia

the current experiment that led to the discovery of the Higgs boson.

Another key concept of SUSY is the idea of R-parity conservation [2]. R-parity is described as

$$\text{R-parity} = (-1)^{2S}(-1)^{3B+L} \tag{1.1}$$

where B and L correspond the baryon and lepton numbers, i.e. the number of baryons and leptons in an interaction, respectively. S is the spin in the interaction. One way of thinking about R-parity is similar to the conservation of energy. In a given interaction, energy is conserved. By imposing R-parity conservation, R-parity is conserved in each interaction.

The main consequence for allowing R-parity is that it guarantees that sparticles (SUSY particles) are produced in pairs. Also, it guarantees that the LSP is stable [2].

My work on the search for SUSY has been studying the application of the novel tool, the quark/gluon discriminator by studying the tool's efficacy and sensitivity to SUSY.

1.2 R-Parity Violating Supersymmetry

The search for SUSY has been an ongoing endeavor, but direct evidence for SUSY has still not been detected. By relaxing one of our criteria for SUSY—the need for R-parity conservation—new decay topologies arise that can be signals for SUSY [2]. Also, RPV SUSY no longer guarantees a stable LSP. While, we lose the dark matter explanation in RPV SUSY, it can still explain the hierarchy problem and the possibility of Grand Unification.

1.3 Stealth SUSY

Another model to consider is Stealth SUSY allowing superpartners to decay through a hidden sector, separate from the SM [8]. Stealth SUSY introduces an extra scalar and its superpartner

into the theory, which are very close in mass, causing the missing energy to be small. The LSP from the superpartner decay is very light, and carries almost no momentum, similar to a neutrino, making events have little to no MET.

1.4 Large Hadron Collider

The LHC collides protons at extremely high energies, allowing us to discover the Higgs boson and possibly superpartners, which are direct evidence for SUSY. The LHC recently upgraded to higher energies from 8 TeV to 13 TeV. However, since we cannot utilize another energy jump to gain an increase in sensitivity and are mostly gathering more data, future progress with current SUSY analysis will be limited by the size of the data set. These data sets from collisions at the LHC allow us to reconstruct events—the recorded detector responses from proton-proton collisions—and analyze jets, which are signatures produced by strongly-interacting quarks and gluons in the form of a cluster of hadrons all moving in a similar direction as seen in **Fig: 4**. This motivates investigating new analysis tools and more sophisticated techniques in order to enhance sensitivities.

The extraordinary energies at the LHC allow us to probe a wide range of energies. One of the key variables in previous searches has been missing transverse momentum (MET) coming from SUSY particles. The MET comes from the lightest supersymmetric particle in the event as it does not interact with the detector, taking away with it momentum. Due to the state of SUSY, a wide variety of models and techniques have been proposed to search for it at both extremes of high MET and low MET. In my thesis, I will discuss the analysis of the efficacy of the quark/gluon discriminator tool for a high MET SUSY search and the aid in development of a search strategy for low MET SUSY models.

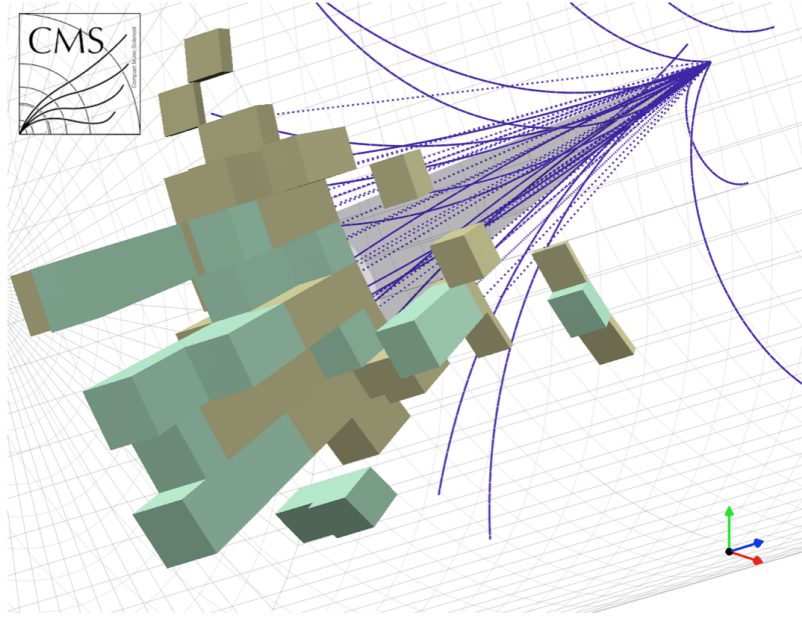


Figure 4: An example of a jet reconstruction in the detectors. Created by CMS.

2 High-MET Searches

2.1 Baseline

One of these realizations looks at gluinos, superpartners of SM gluons. Following **Fig: 5**, the gluinos are produced in pairs as a product of proton-proton collisions, with each decaying into two quarks and an undetected weakly-interacting LSP. Since the LSP has nonzero momentum and energy, then there would be a violation of momentum conservation in the direction of the LSP. The heavier SUSY particles, gluinos, decay rapidly—too fast to observe—so all we observe are the decay products and missing transverse momentum. Also, if the gluinos that decay are heavy, then these would be very energetic events with large transverse momenta.

Hence, the baseline criteria of previous searches is.

- Missing transverse momentum (MET)
- Large scalar sum of jet transverse momenta (H_T)

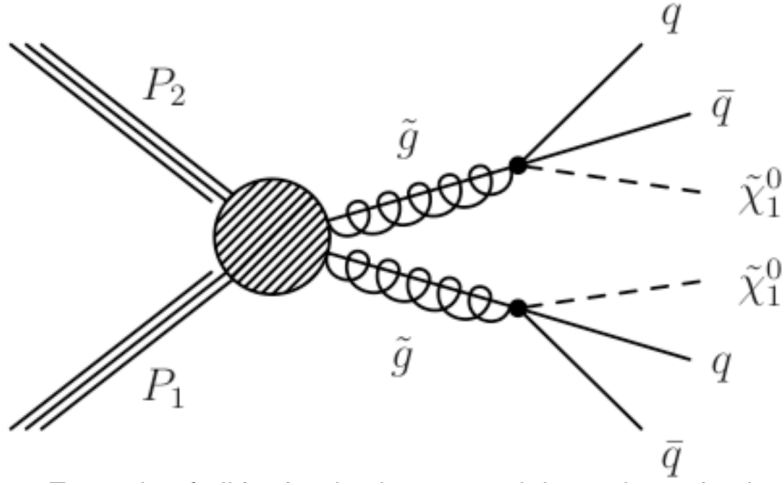


Figure 5: A minimal diagram of an all-hadronic SUSY signal.

- Number of jets (N_{jets})
- Number of b-tagged jets (N_{b-jets}) [10]

A problem arises because the background events can mimic SUSY events by having missing transverse energy and at least four jets, which can be gluon jets that can be produced from protons in the initial state or from radiation of energetic quarks in the decay. Gluon jets can also be produced similarly in the signal events. This is a problem because our signal requires there to be at least four quark jets, but the criteria only requires there to be four jets, not all of them necessarily quark jets. Previous research has enhanced sensitivity by tagging bottom quark jets. However, distinguishing light quark jets from gluon jets is more challenging.

Several background scenarios are prevalent. The top quark pair production mimics this because of its high multiplicity and the missing transverse momentum comes from neutrinos. Another scenario comes from invisible Z^0 decay, where the jets are gluon jets and missing momentum comes from neutrinos. Lastly, another could be that the jets are gluon jets and the missing momentum comes from a mismeasured jet in the detector.

2.2 Quark-Gluon Discriminator

Novel analysis techniques are needed to find evidence for SUSY, if it exists, and to help improve contemporary and future searches. One of these is the quark/gluon discriminator, which discriminates whether a jet is a quark jet or a gluon jet. It especially focuses more on light quark jets.

The discriminator is a multivariate analyzer [5]. It takes 3 variables of the jets as inputs: total multiplicity, second moment minor axis, and how asymmetrical the transverse momentum of a given jet is ($p_T D$). We use total multiplicity because the ratio of the quark and gluon jet multiplicities should converge to a factor especially at high p_T . We expect quark jets to have lower multiplicities compared to gluon jets. The second moment minor axis looks at the pseudorapidity - phi plane. Quark jets are expected to produce narrower jets, so lower values of axes variables compared to gluon jets. Lastly, $p_T D$ is used because quark jets are more likely to produce jets with constituents that have a significant fraction of the jet energy. The discriminator then outputs a value between 0 and 1. From the example histogram in **Fig: 6**, the closer it is to 0, the more likely it is to be a gluon jet, and the closer it is to 1, the more likely it is to be a quark jet.

There have been studies on the efficacy of the quark/gluon discriminator for data at 8 TeV, but not much for the current high energies of the LHC [3]. These studies showed that the discriminator removes 95 percent of the gluon jets, while keeping more than half of the light quark jets [9]. Also, the discriminator has never been used in a hadronic SUSY search before. Therefore, the discriminator can be a powerful tool in enhancing our sensitivities.

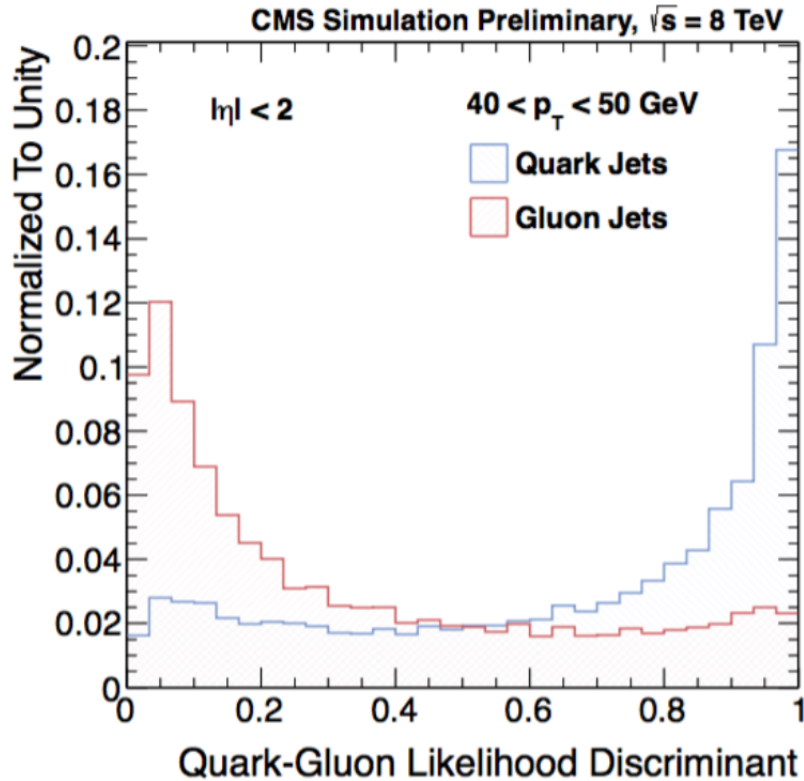


Figure 6: An example of the output of the quark/gluon discriminator [5].

2.3 Methodology

I have studied the application of the discriminator for a hadronic SUSY search using data from the Compact Muon Solenoid (CMS), a detector in the LHC, to improve contemporary and future SUSY searches. At CERN, I analyzed the efficacy of the discriminator and investigated the backgrounds and signals to discern new variables to enhance our sensitivities to SUSY.

To test the efficacy of the discriminator, I used ROOT to apply the discriminator to simulated data, generated using Monte Carlo methods that simulate background and signal events [4]. Since I am analyzing simulated data, I was able to measure the efficacy because the true nature of each jet and each event is known. Also, since I found the more reliable aspect of the discriminator is the portion for quark jets rather than gluon jets, applying a tight cut on the tagger removes more of the gluon jets, without removing many quark jets. The actual values for the cut is: tag gluons

at ≤ 0.1 and tag quarks at ≥ 0.9 .

I investigated the backgrounds and signals by using ROOT to make histograms of the distribution of several key variables, such as number of jets and transverse momentum. I analyzed the shapes of these distributions for the dominant backgrounds and signals at different types of quarks produced and masses of the gluinos and LSPs.

Doing so, I was able to decide on several new variables that utilized the new information. These include the number of quark jets and gluon jets and the H_T fraction for quarks and gluons. We then compare this to the truth of the simulation.

From here, we can enhance the previous selection criteria with the edition of these new variables. Sensitivities are based on number of events of background and signals. We use 2 metrics in units of σ .

$$S \text{ metric} = S/\sqrt{B} \tag{2.1}$$

$$Q = 2(\sqrt{S+B} - \sqrt{B}) \tag{2.2}$$

We then make a cut and observe if sensitivities increase. The sensitivity metric is roughly the expected statistical significance of the signal in standard deviations, assuming it exists. In this field, we treat 3σ as evidence and 5σ as an observation, and the probability that the data are consistent with the background-only hypothesis due to statistical fluctuations is around 3 in a hundred and 1 in a million, respectively.

2.4 Results

The number of quark jets and number of gluon jets are interesting variables to consider as in **Fig: 7**, there is a substantial difference between background events and signal events. Another

variable of interest is the quark HT fraction, but it is not as interesting as seen from the plots in **Fig: 8**. Lastly, another slightly interesting variable is the gluon HT fraction as seen from the plots in **Fig: 9**.

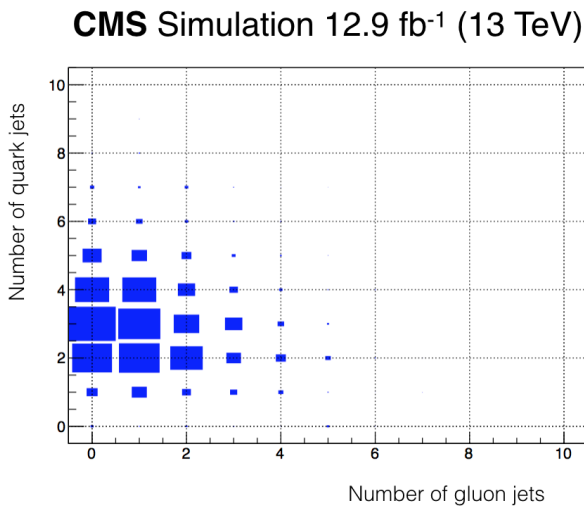
From these new variables, we enhance our previous selection criteria and use show how our sensitivities have increased based on a linear cut in the new variables.

We only considered number of quark jets over number of gluon jets as it is the stronger variable to cut on. From **Fig: 10**, the baseline criteria corresponds to the leftmost point, and the linear cuts on the number of quark jets show the expected increase in the sensitivity to the SUSY signal model.

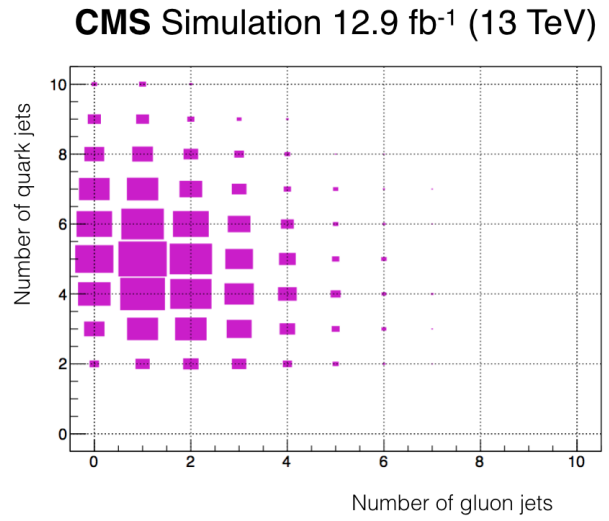
We perform a similar calculation to the quark and gluon HT fraction, seen in **Fig: 11** and **Fig: 12**, respectively. For the quark HT fraction, the baseline selection corresponds to the leftmost point, whereas for the gluon HT fraction, the baseline selection corresponds to the rightmost point. As expected, the sensitivities have increased, but not to the extent of our expectations.

3 Low-MET Searches

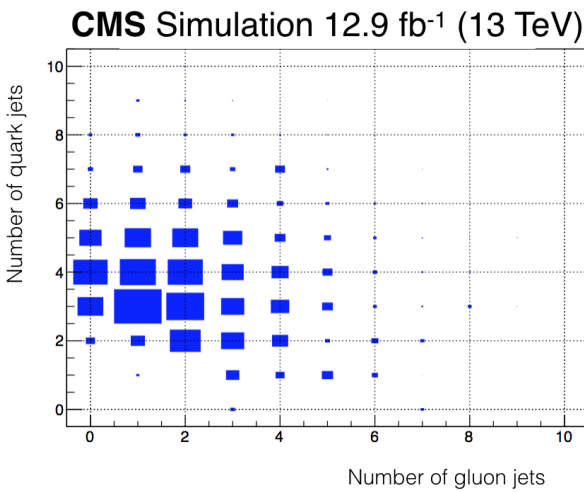
The main difference between R-parity conserving SUSY and R-parity violating (RPV) SUSY is amount missing transverse energy (MET) in our events. Our previous searches for SUSY have been the standard high-MET searches. There could be new physics in low-MET final states. RPV SUSY allows for this as the LSP is no longer stable, allowing for it to decay into SM particles [7]. Stealth SUSY is another interesting model that has the sparticle produced to be extremely light [8]. An analysis to search for a stealth and RPV top squark has final states that include top quarks, many jets, no MET, so this final state is quite general.



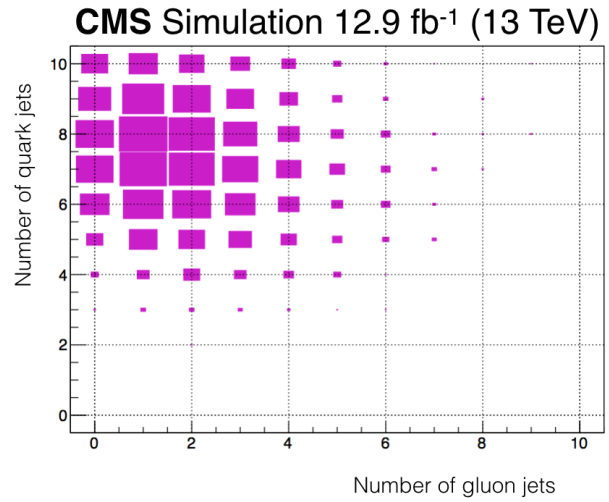
(a) Number of quark jets vs. number of gluon jets for background events



(b) Number of quark jets vs. number of gluon jets for signal events

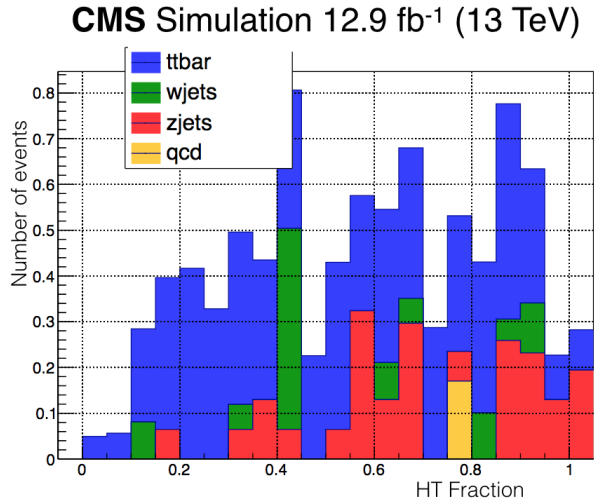


(c) True number of quark jets vs. true number of gluon jets for background events.

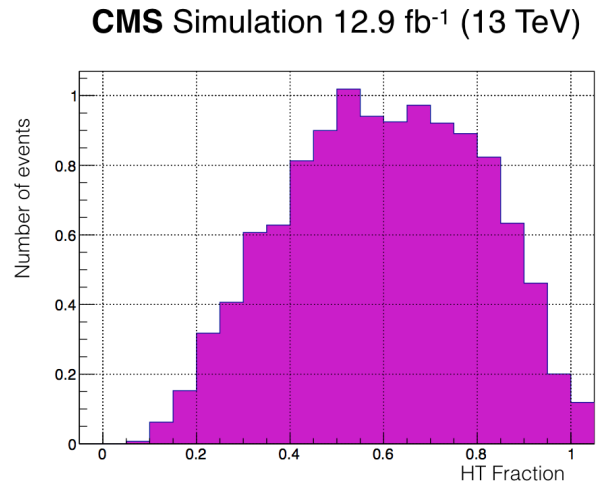


(d) True number of quark jets vs. true number of gluon jets for signal events.

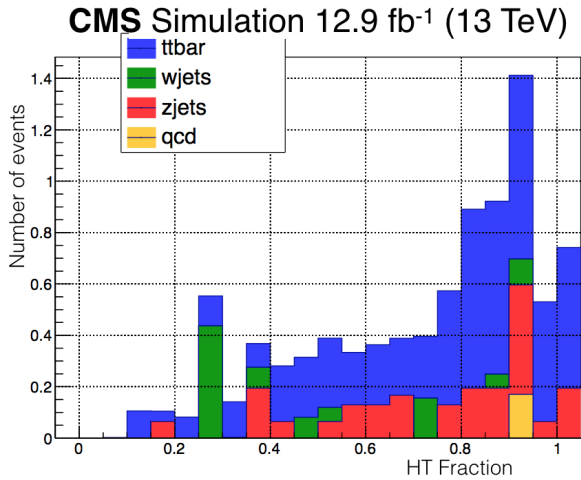
Figure 7: A comparison of the different plots of number of quark jets vs. number of gluon jets to see which cut is the most optimal.



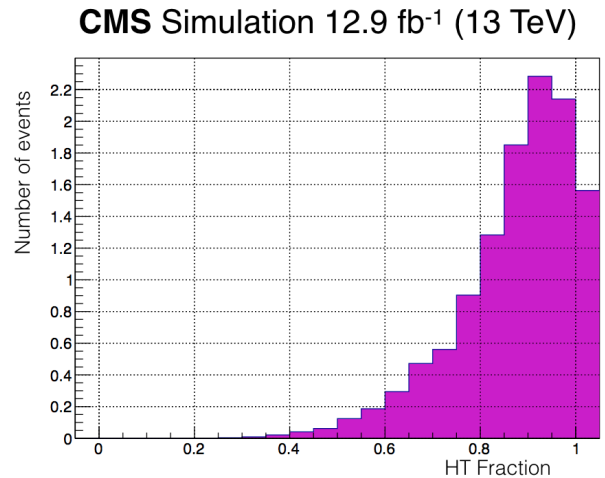
(a) Quark HT fraction for background events.



(b) Quark HT fraction for signal events.

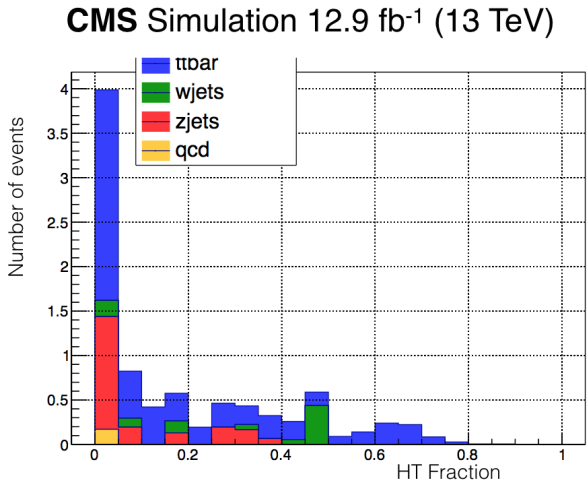


(c) True quark HT fraction for background events.

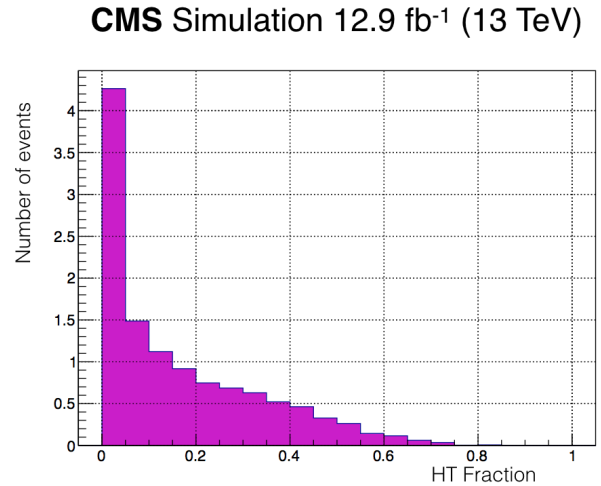


(d) True quark HT fraction for signal events.

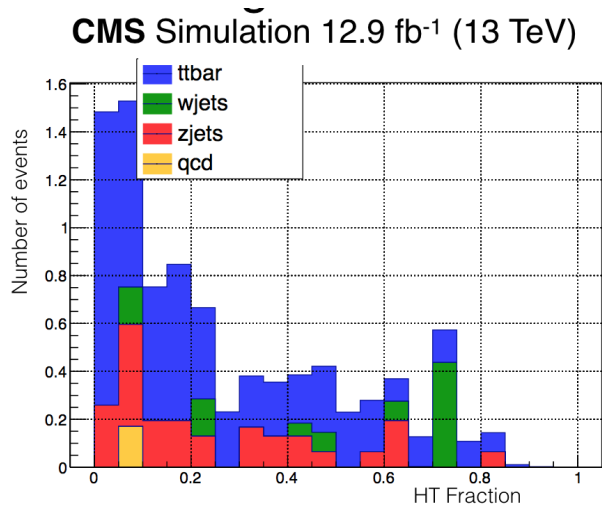
Figure 8: A comparison of the topologies of the different types of Quark HT fraction to observe which cut is most optimal.



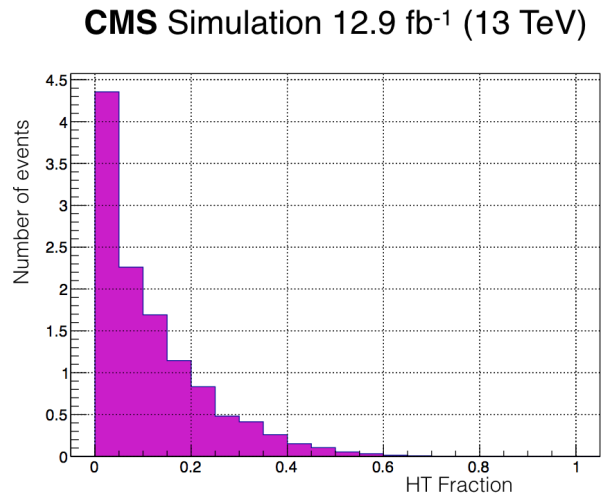
(a) gluon HT fraction for background events.



(b) gluon HT fraction for signal events.



(c) True gluon HT fraction for background events.



(d) True gluon HT fraction for signal events.

Figure 9: A comparison of the topologies of the different types of gluon HT fraction to observe which cut is most optimal.

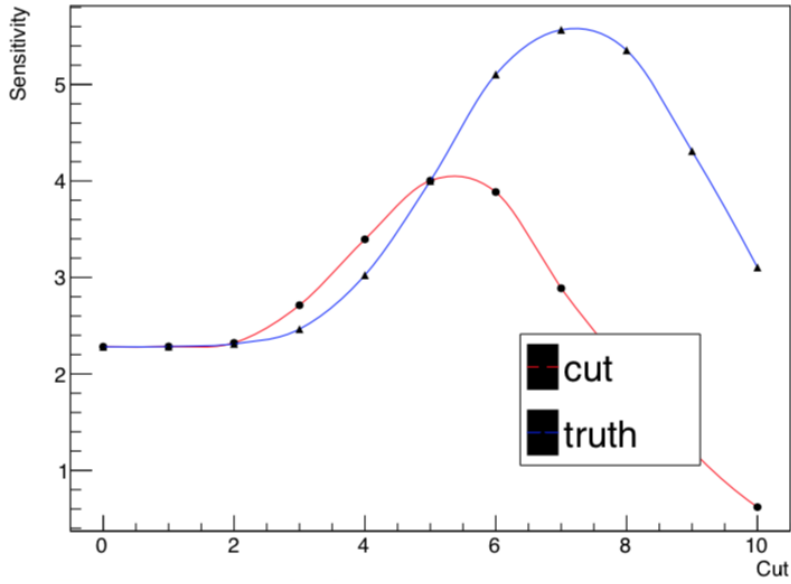
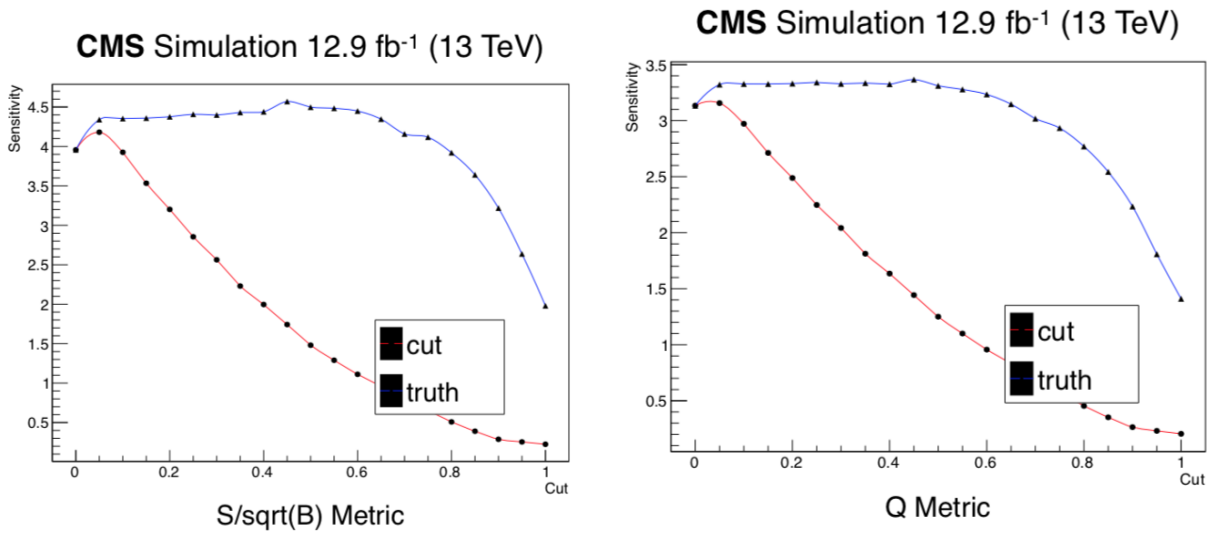


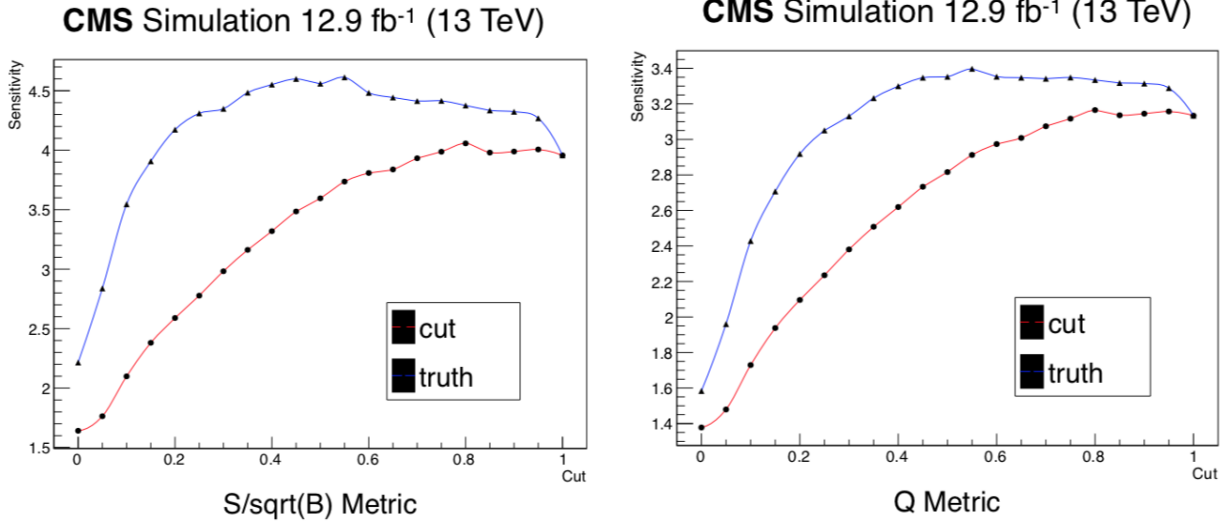
Figure 10: The S metric for linear cuts on number of quark jets. The red lines correspond to the discriminator and the blue lines correspond to the truth values from the simulations.



(a) S metric for quark HT fraction

(b) Q metric for quark HT fraction

Figure 11: The S and Q metrics for linear cuts on quark HT fraction. The red lines correspond to the discriminator and the blue lines correspond to the truth values from the simulations.



(a) S metric for gluon HT fraction

(b) Q metric for gluon HT fraction

Figure 12: The S and Q metrics for linear cuts on gluon HT fraction. The red lines correspond to the discriminator and the blue lines correspond to the truth values from the simulations.

3.1 Event Topologies

For the Stealth SYY topology, the proton-proton collision generates two top squarks and decays as in **Fig: 13**. Each top squark then decays into a gluon, top quark, and a squark. This subsequent squark then decays into the SM equivalent quark and a gravitino—the LSP. The quark then decays into two gluons. Given two top squarks, then the final state of this scenario is two top quarks and six jets.

For the Stealth SH_uH_d topology, the proton-proton collision again generates two top squarks and decays as in **Fig: 14**. Each top squark then decays into a squark and top quark. The squark then decays into a quark and a gravitino. In this version, the quark then decays into two bottom quarks. Given two top squarks, then the final state of this scenario is two top quarks and 4 bottom quarks.

For the RPV UDD topology, the proton-proton collision again generates two top squarks and

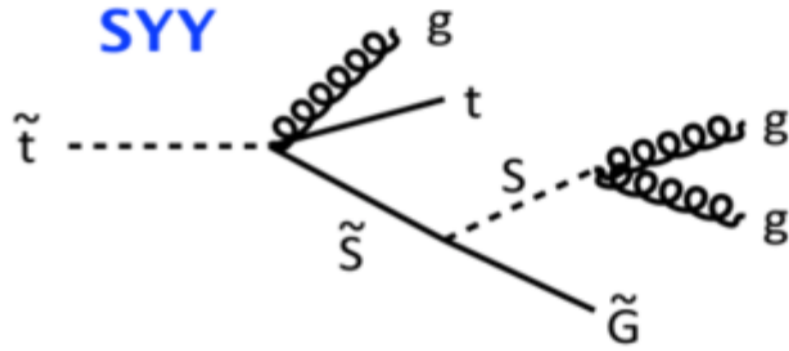


Figure 13: The event topology for a top squark decay for Stealth SYY model

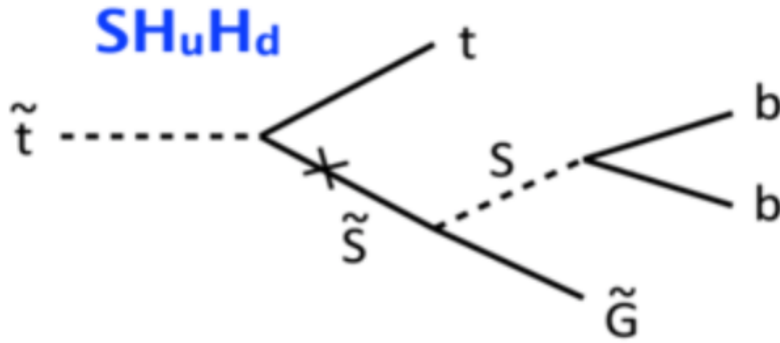


Figure 14: The event topology for a top squark decay for the Stealth $SH_u H_d$ model.

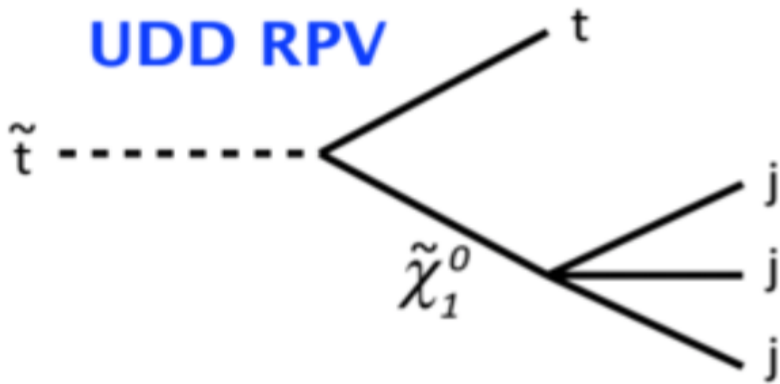


Figure 15: The event topology for a top squark decay for the RPV UDD model.

decays as in **Fig: 15**. Each top squark then decays into a top quark and a chargino/neutralino—the LSP, which then decays into 3 quarks. Given two top squarks, the final state of this scenario is two top quarks and six jets.

3.2 Search Strategy

We will consider both 0 lepton and 1 lepton categories to maximize our sensitivity. Unlike the high-MET searches as shown above, we consider top quarks that can decay leptonically, so we expect there to be an electron or a muon in our events as well.

So our event selection for 0 leptons is

- $HT > 500GeV$
- At least 6 jets with $p_T > 45GeV$
- At least one b-tagged jet
- 0 leptons
- At least one hadronic top quark

In this event selection, the main background come from $t\bar{t}$ and QCD production.

Our event selection for 1 lepton is

- 1 electron or muon with $p_T > 30GeV$
- At least 6 jets with $p_T > 30GeV$
- At least one b-tagged jet
- One leptonic top quark—a top decay into a bottom, charged-lepton, and a neutrino.

The reason for the energies of the jets being less compared to 0 lepton, is that the jets are less energetic in these types of events. In this event selection, the main background is $t\bar{t}$ production.

3.3 1 Lepton Search

For these searches, I have been focused on data selection. One of the ways to better understand our signal models is to compare our data to what Monte Carlo simulations look like. This was done by analyzing the event shapes of key variables of the events. These key variables, especially the jet momentum tensor and Fox Wolfram moments.

The jet momentum tensor is defined as the 3×3 matrix

$$S^{\alpha,\beta} = \frac{\sum_i p_i^\alpha p_i^\beta}{\sum_j |p_j|^2} \quad (3.1)$$

where the indices α and β are the Cartesian directions and the sums are over the jets in the events. From this matrix, we calculate the eigenvalues λ_1 , λ_2 , and λ_3 . These eigenvalues tells us about the distributions of the jets in our events. The event has an isotropic distribution if the eigenvalues have similar values. The event has a planar distribution, if one of the eigenvalues is significantly smaller than the others. Lastly, the event has a di-jet topology—one jet going one direction and another going in the opposite direction—if one is large and two are significantly smaller.

The other variables are the Fox Wolfram moments which are defined as

$$H_l = \sum_{i,j} |p_i||p_j|P_l(\cos\theta_{ij}) \quad (3.2)$$

where P_l are the Legendre polynomials. The double sums over all pairs of jets including $i = j$. Similar to the eigenvalues of the jet momentum tensor, the values of the Fox Wolfram moments greatly differ depending on the type of event.

This portion of the study was done using the baseline selection as described above for a 1 lepton search, with an additional precautionary selection of events with less than or equal to 8 jets. When

performing an analysis, before we fully run our code over all the data, we make sure that we are blinded, so that we are not biased in the results. As we expect the signals to have a large amount of jets, > 10 , by adding this precautionary criteria, we are certain that we are only analyzing the events coming from the background.

3.3.1 Data/MC

However, while making data and Monte Carlo comparisons, the ratios of the expected events are a bit off when studying the event shapes of these variables in the 1 lepton selection. One of the ways to further study this is checking the p_T and the pseudorapidity, η , of the most energetic lepton to check for the localization in the inefficiency of the data, as done in **Figs: 16, 17, 18, and 19**.

3.3.2 Trigger Efficiencies

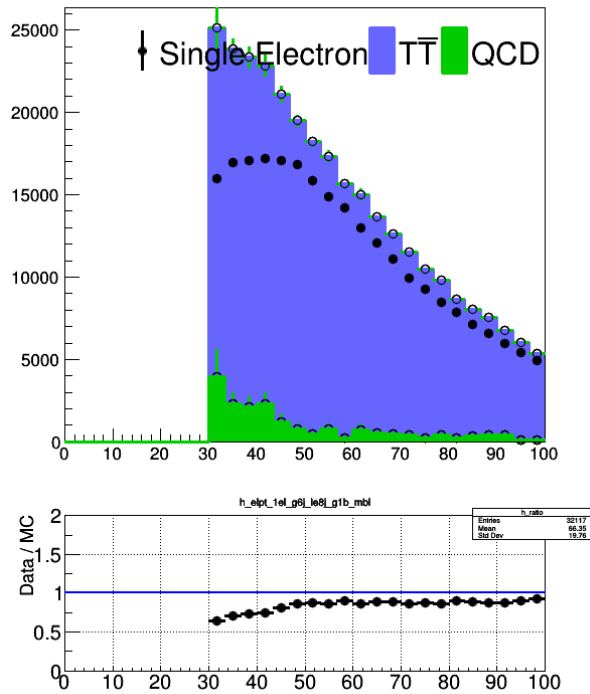
From these plots, the difference in data and Monte Carlo, can come from the trigger efficiency. The triggers are used when the detector is taking data. As there are billions of collisions per second, there will be many events that are not interesting. In order to keep the interesting events, we use triggers that keep events with certain properties. The obvious next step is to study the triggers that we have used to select the events in our data.

The data sets that we are interested in are events with a single electron and events with a single muon. For these data sets, certain triggers were required for it to be passed.

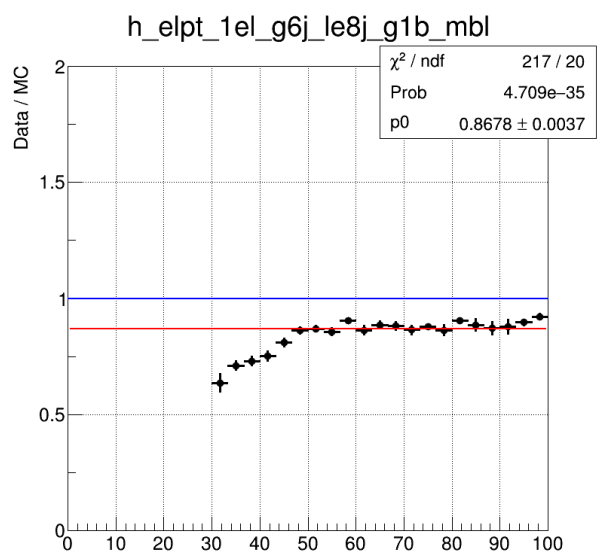
For Single Electron data sets:

- HLT_Ele27_WPTight_Gsf_v
- HLT_Ele45_WPLoose_Gsf_v

For Single Muon data sets:

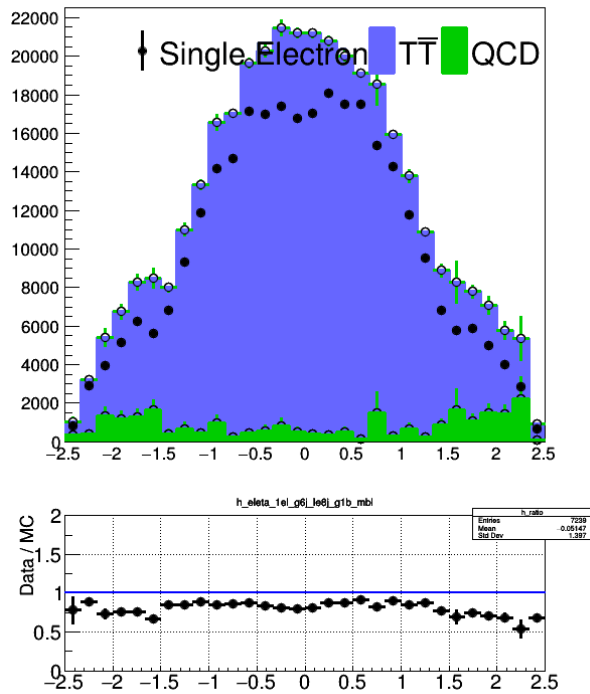


(a) CMS Work in Progress

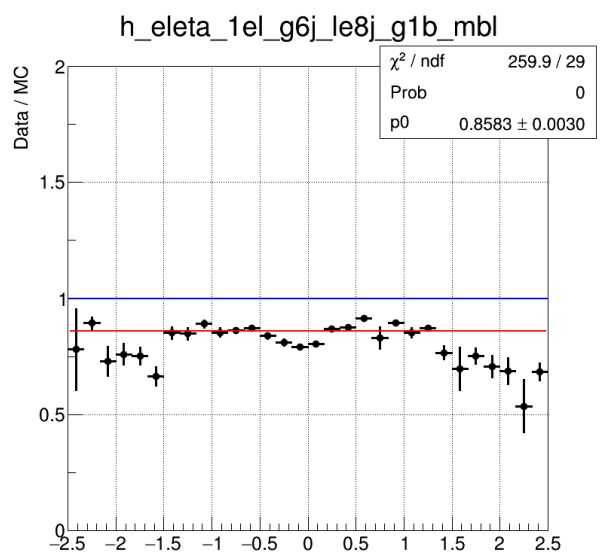


(b) CMS Work in Progress

Figure 16: The leading electron p_T for the Single Electron data set plotted against the background events. The one on the right is an enhancement of the ratio plot. The red line corresponds to the best fit 0th order function.

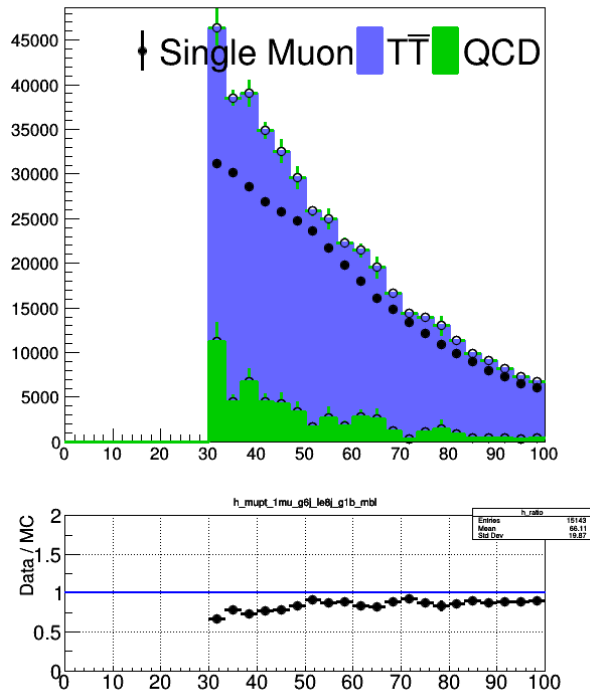


(a) CMS Work in Progress

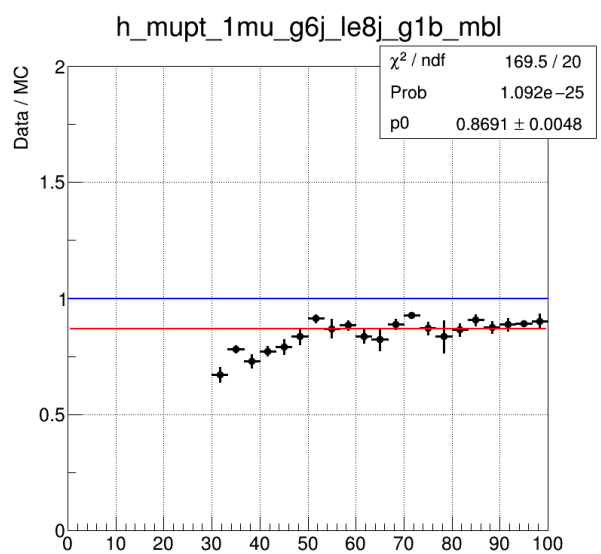


(b) CMS Work in Progress

Figure 17: The leading electron η for the Single Electron data set plotted against the background events. The one on the right is an enhancement of the ratio plot. The red line corresponds to the best fit 0th order function.

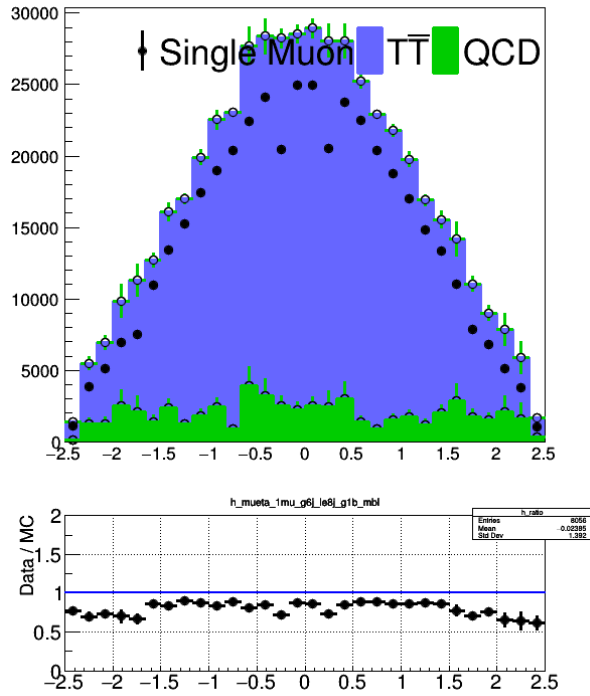


(a) CMS Work in Progress

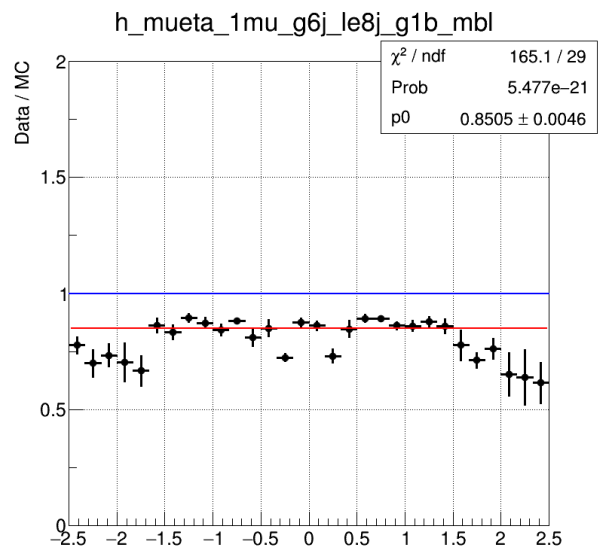


(b) CMS Work in Progress

Figure 18: The leading muon p_T for the Single Muon data set plotted against the background events. The one on the right is an enhancement of the ratio plot. The red line corresponds to the best fit 0th order function.



(a) CMS Work in Progress



(b) CMS Work in Progress

Figure 19: The leading muon η for the Single Muon data set plotted against the background events. The one on the right is an enhancement of the ratio plot. The red line corresponds to the best fit 0th order function.

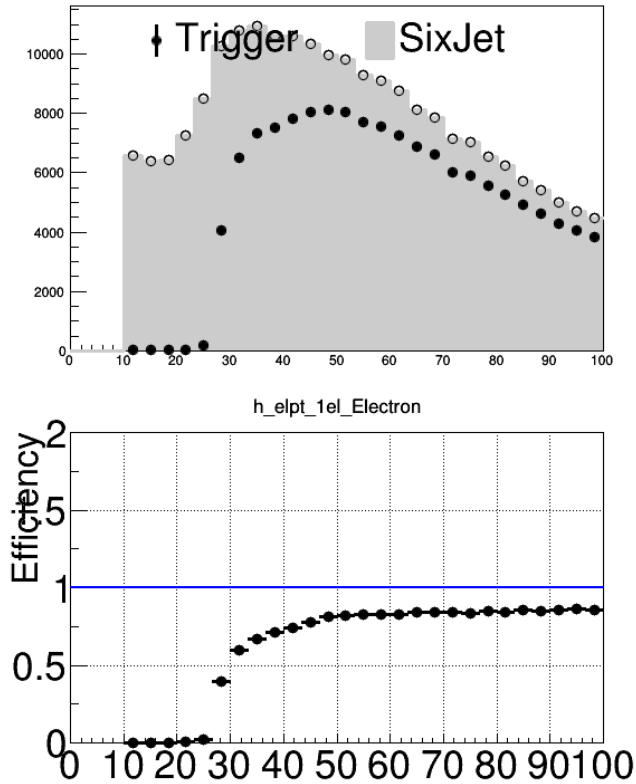


Figure 20: **CMS Work in Progress:** The leading electron p_T for the six jet data set. The gray is the whole data set, and the black points are those that pass the trigger. The bottom plot is the efficiency plot with the value being the ratio between the black points and the gray points. These are plotted for a combination of all triggers.

- HLT_IsoMu22_eta2p1_v
- HLT_IsoMu22_v
- HLT_IsoTkMu22_v
- HLT_IsoTkMu24_v
- HLT_Mu45_eta2p1_v
- HLT_Mu50_v
- HLT_TkMu50_v

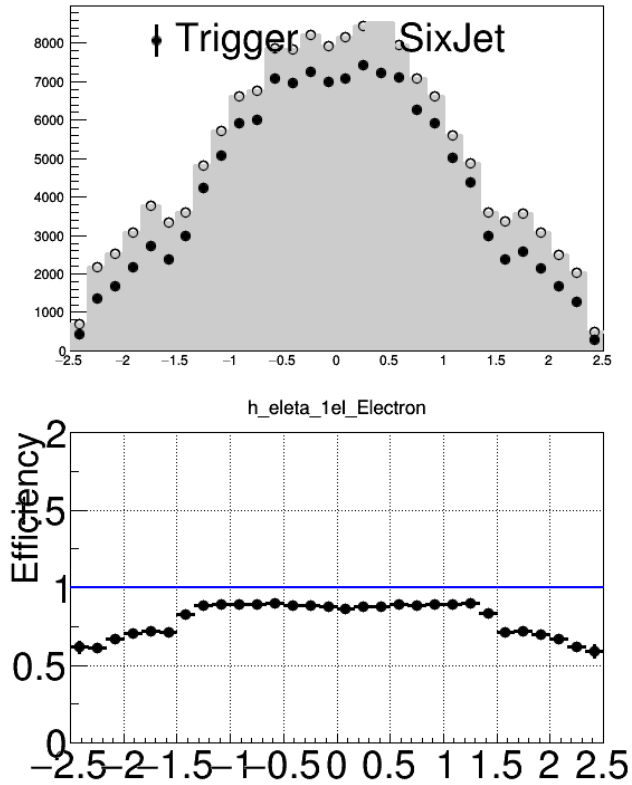


Figure 21: **CMS Work in Progress:** The leading electron η for the six jet data set. The gray is the whole data set, and the black points are those that pass the trigger. The bottom plot is the efficiency plot with the value being the ratio between the black points and the gray points. These are plotted for a combination of all triggers.

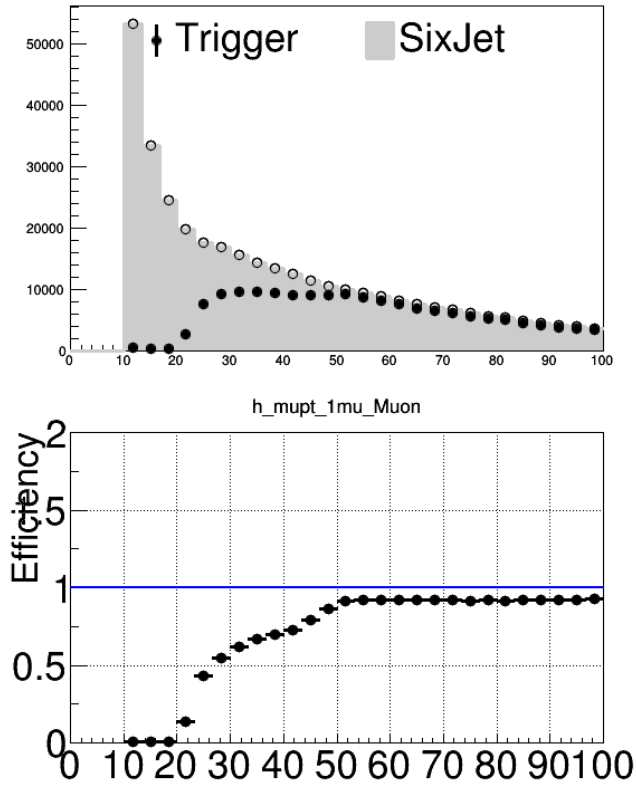


Figure 22: **CMS Work in Progress:** The leading muon p_T for the six jet data set. The gray is the whole data set, and the black points are those that pass the trigger. The bottom plot is the efficiency plot with the value being the ratio between the black points and the gray points. These are plotted for a combination of all triggers.

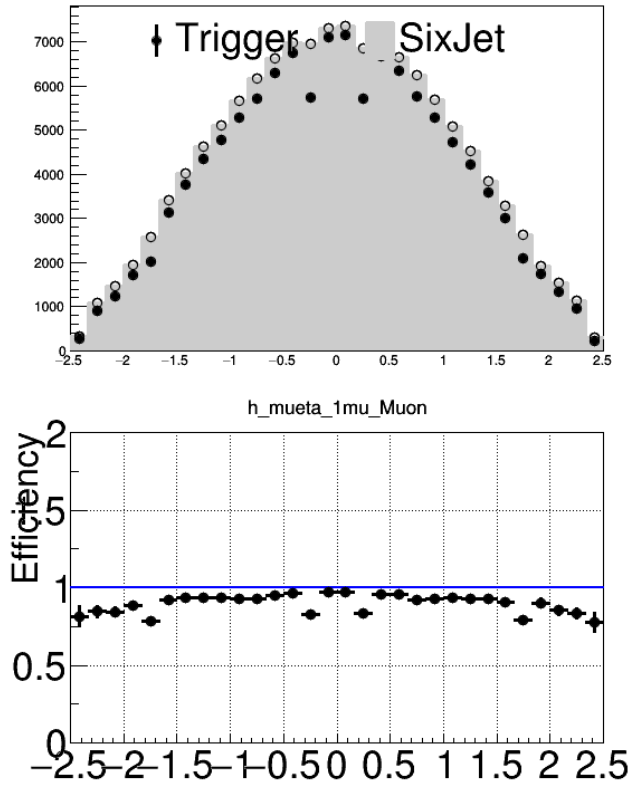


Figure 23: **CMS Work in Progress:** The leading muon η for the six jet data set. The gray is the whole data set, and the black points are those that pass the trigger. The bottom plot is the efficiency plot with the value being the ratio between the black points and the gray points. These are plotted for a combination of all triggers.

From analyzing the efficiencies in **Figs: 20, 21, 22, and 23**, we see that the inefficiency occurs when the jets are particularly soft— $< 50\text{GeV}$. We diagnose that this is because of the isolation requirements of these triggers.

4 Conclusion

By studying both extremes of the key variable, missing transverse momentum (MET), we are able to study a wide range of different SUSY models. From my analysis on the efficacy of the quark/gluon discriminator, I found that the tool has increased our sensitivities to SUSY for some signal models. However, I also found that there are significant differences between the discriminator and the truth from the Monte Carlo simulation. With perfect discrimination, we can significantly increase our sensitivities compared of the current discriminator and to many more signal models. These improvements can be explored in the future, using machine learning. From developing a search strategy for the low MET SUSY models, I focused on trigger efficiencies to see which are the optimal triggers to use in this type of search.

References

- [1] P. A. R. Ade et al. Planck 2013 results. I. Overview of products and scientific results. *Astron. Astrophys.*, 571:A1, 2014.
- [2] R. Barbier et al. R-parity violating supersymmetry. *Phys. Rept.*, 420:1–202, 2005.
- [3] R. Michael Barnett, John F. Gunion, and Howard E. Haber. Gluino Decay Patterns and Signatures. *Phys. Rev.*, D37:1892, 1988.
- [4] R. Brun and F. Rademakers. ROOT: An object oriented data analysis framework. *Nucl. Instrum. Meth.*, A389:81–86, 1997.
- [5] CMS Collaboration. Performance of quark/gluon discrimination in 8 TeV pp data. 2013.
- [6] S. Dimopoulos, S. Raby, and Frank Wilczek. Super-

- symmetry and the Scale of Unification. *Phys. Rev.*, D24:1681–1683, 1981.
- [7] Jared A. Evans and Yevgeny Kats. LHC Coverage of RPV MSSM with Light Stops. *JHEP*, 04:028, 2013.
- [8] JiJi Fan, Rebecca Krall, David Pinner, Matthew Reece, and Joshua T. Ruderman. Stealth Supersymmetry Simplified. *JHEP*, 07:016, 2016.
- [9] Jason Gallicchio and Matthew D. Schwartz. Quark and Gluon Tagging at the LHC. *Phys. Rev. Lett.*, 107:172001, 2011.
- [10] Vardan Khachatryan et al. Search for supersymmetry in the multijet and missing transverse momentum final state in pp collisions at 13 TeV. *Phys. Lett.*, B758:152–180, 2016.
- [11] Stephen P. Martin. A Supersymmetry primer. pages 1–98, 1997. [Adv. Ser. Direct. High Energy Phys.18,1(1998)].